Decrease of sialic acid residues as an *eat-me* signal on the surface of apoptotic lymphocytes

Hanna Marie Meesmann[1], Eva-Marie Fehr[1], Sonja Kierschke[1], Martin Herrmann[2], Rostyslav Bilyy[3], Petra Heyder[1], Norbert Blank[1], Stefan Krienke[1], Hanns-Martin Lorenz[1] and Martin Schiller[1,*]

[1]Department of Medicine V, University of Heidelberg, Im Neuenheimer Feld 410, 69120 Heidelberg, Germany
[2]Institute for Clinical Immunology and Rheumatology, Department of Internal Medicine 3, University Hospital Erlangen, 91054 Erlangen, Germany
[3]Institute of Cell Biology, National Academy of Sciences of Ukraine, Drahomanov Street 14/16, 79005 Lviv, Ukraine
*Author for correspondence (martin.schiller@med.uni-heidelberg.de)

Accepted 14 June 2010
Journal of Cell Science 123, 3347-3356

doi:10.1242/jcs.066696

Summary

The silent clearance of apoptotic cells is essential for cellular homeostasis in multicellular organisms, and several mediators of apoptotic cell recognition have been identified. However, the distinct mechanisms involved are not fully deciphered yet. We analyzed alterations of the glycocalyx on the surfaces of apoptotic cells and its impact for engulfment. After apoptosis induction of lymphocytes, a decrease of α2,6-terminal sialic acids and sialic acids in α2,3-linkage with galactose was observed. Similar changes were to be found on the surface of apoptotic membrane blebs released during early stages of apoptosis, whereas later released blebs showed no impaired, but rather an increased, exposure of sialic acids. We detected an exposure of fucose residues on the surface of apoptotic-cell-derived membrane blebs. Cleavage by neuraminidase of sialic acids, as well as lectin binding to sialic acids on the surfaces, enhanced the engulfment of apoptotic cells and blebs. Interestingly, even viable lymphoblasts were engulfed in an autologous cell system after neuraminidase treatment. Similarly, the engulfment of resting apoptotic lymphocytes was augmented after neuraminidase treatment. However, the engulfment of resting viable lymphocytes was not significantly enhanced after neuraminidase treatment. Our findings support the importance of the glycocalyx, notably the terminal sialic acids, in the regulation of apoptotic cell clearance. Thus, depending on cell type and activation status, changes in surface glycosylation can either directly mediate cellular engulfment or enhance phagocytosis by cooperation with further engulfment signals.

Key words: Apoptosis, Clearance, Glycocalyx, Lectin, Sialic acid

Introduction

The surface of all human cells is characterized by a prominent sugar coat referred to as glycocalyx. Sugar chains occur nearly exclusively at the outer membrane leaflet and are covalently linked to membrane proteins or lipids. The synthesis of the glycocalyx starts in the endoplasmic reticulum (ER), where sugar molecules are attached to membrane components. These premature membranes are further modified within the Golgi and finally transported to the cellular surface. Here, the glycocalyx plays an important role in several cellular functions such as cell-to-cell communication, cell–matrix interaction or recognition of self and non-self (Flotenmeyer et al., 1999; Kottgen et al., 2003).

Well-studied members of the cell-surface sugars are the *N*-acetyl neuraminic acids, also called sialic acids (Sias), which are nine-carbon monosaccharides, bear a negative charge and are most commonly found at the non-reducing terminal positions of *N*- and *O*-glycans. This prominent position as well as their negative charge means that Sias are involved in a variety of functions (Varki, 1993).

The biosynthesis of membrane sialylated glycoproteins is catalyzed by a group of enzymes called sialyltransferases (Tsuji et al., 1996), which are part of the Golgi membrane-bound glycosyltransferases. These enzymes transfer Sias to β-D-galactopyranosyl residues via α2,3- or α2,6-linkages, or to β-D-*N*-acetylgalactosaminyl and β-D-*N*-acetylglucosaminyl residues via α2,6-linkages (Harduin-Lepers et al., 2001). Once exposed at the cellular surface, Sias can be removed by sialidases, also referred to as neuraminidases (NEU). In human, four sialidases have been identified and classified according to their subcellular localization: the lysosomal NEU-1, the cytosolic NEU-2, the plasma-membrane-associated NEU-3 and the lysosomal/mitochondrial NEU-4 (Monti et al., 2002; Zanchetti et al., 2007). These membrane-bound enzymes enable modification of the membrane sugar composition and thus take part in signal transduction.

Various constituents of the glycocalyx are recognized by a group of sugar-binding proteins called lectins (Sharon and Lis, 2004). Human lectins are divided into different groups, depending on their structural diversities. C-type lectins (e.g. mannose-binding lectin, pulmonary surfactant, macrophage mannose receptor, DC-SIGN) bind their ligands in a calcium-dependent manner. Galectins are specific for β-galactosides. I-type lectins, which belong to the family of immunoglobulins, include the Sia-specific group of siglecs (Kottgen et al., 2003). These lectins are involved in pathogen recognition, complement activation, immunomodulation, cell adhesion and migration (Crocker et al., 2007).

Beside these varying physiological functions, lectins have attracted attention as helpful tools for the characterization of the carbohydrate profile on cells. We used the following plant lectins and their specificity for particular carbohydrates for the characterization of the glycocalyx: Ulex europaeus agglutinin I (UEA-I) binding to α-linked fucose residues (Allen et al., 1977); Griffonia simplicifolia lectin II (GSL-II) binding to *N*-acetyl-glucosamine (Hennigar et al., 1986); Sambucus nigra agglutinin (SNA) binding α2,6-Sia residues; and Maackia amurensis lectin I

(MAL-I) binding to Sias linked to galactose (Gal) with an α2,3-linkage (Knibbs et al., 1991; Wang and Cummings, 1988).

In the last few decades, the glycocalyx has attracted attention especially in the context of apoptosis and the clearance of apoptotic cells. In addition to well-known mediators of apoptotic cell engulfment, such as phosphatidylserine (PS) (Fadok et al., 2000), brain-specific angiogenesis inhibitor 1 (BAI1) (Park et al., 2007), T-cell immunoglobulin- and mucin-domain-containing molecule 4 (Tim4) (Miyanishi et al., 2007), growth-arrest-specific gene-6 (GAS6) (Wu et al., 2006) or milk fat globule-EGF factor 8 (Mfge8) (Kranich et al., 2008), some authors have reported that changes in the glycoprofile influence the phagocytosis of apoptotic cells. Here, amongst others, galectins (Beer et al., 2008), C-type lectins (Cambi and Figdor, 2003), CD43 (van den Berg et al., 2001) and the asialoglycoprotein receptor (Ashwell and Morell, 1974) are reportedly involved.

In this study, we observed an altered composition of the glycocalyx on the surfaces of apoptozing cells. In parallel, we characterized changes in the surface glycosylation of apoptotic cellular membrane blebs. These alterations are characterized by a decrease in terminal α2,6-linked Sias and Sia-α2,3-Gal residues on the cellular surface. Furthermore, we observed an initial decrease of terminal Sias and galactose linked Sias on apoptotic membrane blebs. However, during later stages of apoptosis, Sias were rather increased on the surface of apoptotic membrane blebs. Moreover, we observed the exposure of fucose residues on apoptotic-cell-derived membrane blebs. These glycocalyx alterations enhance the engulfment of apoptotic as well as viable lymphoblasts. Analysis of resting lymphocytes showed that desialylation caused an enhanced uptake of apoptotic cells, whereas engulfment of viable cells was not affected.

Results

Induction of apoptosis in activated lymphoblasts causes a decrease of α2,3- and α2,6-linked sialic acids on the cell surface

Apoptosis was induced in lymphoblasts by UV-B irradiation or treatment with staurosporine (STS) and subsequently analyzed by flow cytometry. To quantify apoptotic cells, we analyzed morphological changes [cellular shrinkage, side scatter (SSC) increase] as well as exposure of PS on the outer membrane leaflet. As shown in Fig. 1A, UV-B and STS treatment caused an increase of AnnexinV (AxV)-positive cells as well as characteristic morphological changes [forward scatter (FSC)/SSC characteristics]. The first changes occurred at 4–8 hours after induction of apoptosis and statistically significant changes were to be observed at 24 and 48 hours. IL-2-stimulated lymphoblasts served as viable controls.

We then analyzed the binding of FITC-labelled plant lectins (MAL-I, SNA, UEA-I, GSL-II) to the cellular surface to quantify changes of the glycocalyx during apoptosis. Importantly, a high staining for all lectins to intracellular membranes was detected when we analyzed secondary or primary necrotic cells. Thus, the staining of intracellular membranes (which show a different, immature glycosylation pattern) must strictly be excluded during analysis of the glycocalyx alterations on cellular surfaces. To eliminate artefacts due to intracellular binding of lectins, propidium iodide (PI)-positive (necrotic) cells with permeable membranes were excluded in flow cytometry.

Analyzing lectin binding to the surface of cells treated with UV-B or STS, we observed a significant decrease of SNA and MAL-I binding of apoptotic cells (24 and 48 hours after induction). SNA and MAL-I showed a rather high binding to viable lymphoblasts (Fig. 1B). Thus, apoptozing cells showed a decreased exposure of terminal α2,3- and α2,6-linked sialic acids. GSL-II (binding *N*-acetylglucosamine) and UEA-I (binding terminal fucose if accessible) barely stained viable lymphoblasts and we did not observe any significant alterations after the induction of apoptosis. The time course of changes in lectin binding to apoptotic cells was further analyzed and AxV staining was performed in parallel. A first decrease of MAL-I and SNA binding was observed at 4–8 hours after apoptosis induction, and changes were statistically significant after 24 and 48 hours of incubation. This decrease in surface sialylation occurred simultaneously with an increase in PS exposure on the outer membrane leaflet (Fig. 1C,D).

Lectin binding was further analyzed by confocal microscopy (Fig. 2). Apoptotic lymphoblastss were stained with FITC-labelled lectins and PE-conjugated ER-tracker to visualize all cells, irrespective of their lectin-binding capacity. In confocal microscopy, a clear surface staining of apoptotic cells by MAL-I and SNA was detected. For GSL-II and UEA-I, we observed no binding to apoptotic cells in confocal microscopy images (Fig. 2). In these experiments, we also observed a binding of SNA and MAL-I to apoptotic-cell-derived membrane blebs and the process of apoptotic cell blebbing was visualized very well by SNA and MAL-I staining (see arrowheads in Fig. 2). Most interestingly, apoptotic-cell-derived membrane blebs were stained by UEA-I (see arrows in Fig. 2), whereas apoptotic cells appeared almost unstained.

We further investigated lectin binding to apoptotic-cell-derived membrane blebs. These membrane-coated vesicles are released during apoptosis by plasma membrane blebbing and their size and content have been described by various groups in the last few years (Cline and Radic, 2004; Miguet et al., 2006; Schiller et al., 2008). Apoptotic-cell-derived membrane blebs were isolated as described previously (Schiller et al., 2008), stained by MAL-I, SNA, UEA-I or GSL-II, and analyzed by flow cytometry. Interestingly, we observed a high binding of MAL-I and SNA immediately after induction of apoptosis and a decrease of MAL-I and SNA binding during early stages of apoptotic cell death (up to 8 hours after apoptosis induction) (Fig. 3A). By contrast, apoptotic cell blebs released during later stages of apoptosis (24 and 48 hours) showed no impaired or even an increased binding of MAL-I and SNA (Fig. 3A, Fig. 3B). UEA-I slightly stained apoptotic membrane blebs and no binding of GSL-II was observed in flow cytometry.

Sialic-acid-binding plant lectins enhance phagocytosis of apoptotic cells and apoptotic-cell-derived membrane blebs

Next, we were interested in whether alterations of the glycocalyx play a role in the engulfment of apoptotic cells and apoptotic-cell-derived membrane blebs. To analyze this, we pretreated apoptotic cells as well as apoptotic-cell-derived membrane blebs by MAL-I, SNA, UEA-I and GSL-II. Subsequently, cells and blebs were washed, and then co-cultured together with monocyte-derived phagocytes. Engulfment of apoptotic cells and apoptotic-cell-derived membrane blebs was assessed by confocal microscopy. As shown in Fig. 4, incubation of apoptotic cells together with the Sia binding lectins MAL-I and SNA considerably enhanced the engulfment of apoptotic cells by monocyte-derived phagocytes (Fig. 4). By contrast, addition of UEA-I or GSL-II to apoptotic cells before co-culture with monocyte-derived phagocytes did not influence apoptotic cell engulfment (not shown).

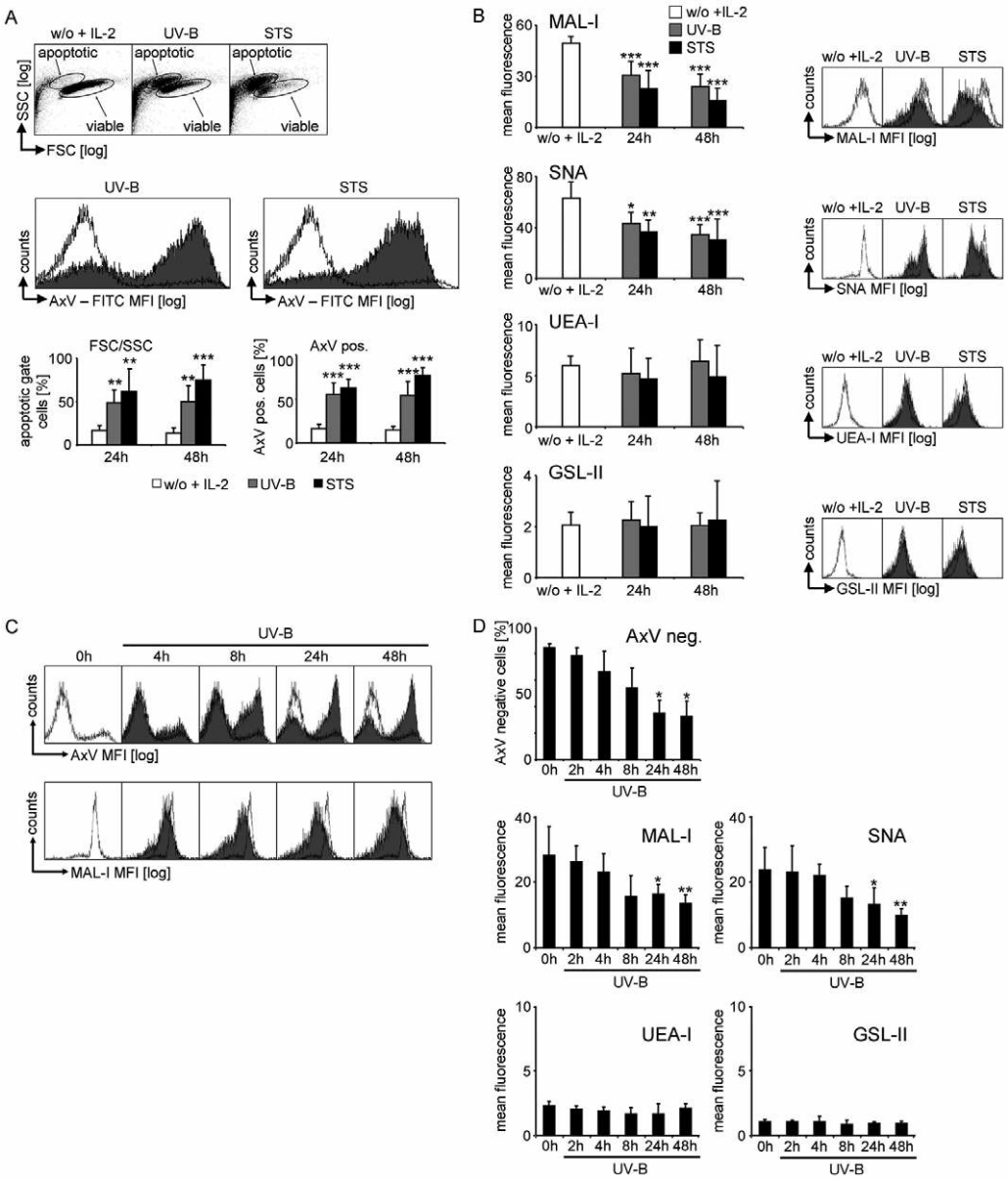

Fig. 1. Quantification of apoptosis and changes in the glycocalyx. (**A**) Quantification of apoptosis by flow-cytometry. Activated lymphoblasts were analyzed after apoptosis induction by UV-B irradiation (90 mJ/cm^2) or STS treatment (0.1 μM; incubation for 24 hours). Viable controls were incubated with IL-2 (w/o + IL-2). Top: dot plots show FSC/SSC-properties of viable and apoptotic cells. Middle: AxV–FITC fluorescence (open graphs are from viable controls and shaded graphs from apoptotic cells). PI-positive cells were excluded. Bottom: bar graphs summarize data obtained from six independent experiments (incubation for 24 and 48 hours). Left: percentage of cells found in the apoptotic cell gate (see upper dot plots). Right: percentage of AxV-positive cells. (**B**) Analysis of lectin binding to apoptotic lymphoblasts. Lymphoblasts were stained with FITC-labelled lectins MAL-I, SNA, UEA-I and GSL-II 24 and 48 hours after induction of apoptosis. Left: data obtained from seven independent experiments. Right: corresponding original data obtained from one representative experiment (24 hours incubation). The open graphs are from viable controls and the shaded graphs from apoptotic cells. (**C**) Kinetics of AxV binding and MAL-I binding to apoptotic lymphoblasts. Apoptosis was induced by UV-B treatment, and flow cytometry was performed after the indicated incubation periods. The open graphs are from viable controls and the shaded graphs from apoptotic cells. Lymphoblasts were stained with FITC-labelled AxV or the lectin MAL-I. Above: AxV–FITC fluorescence. Below: MAL-I fluorescence. PI-positive cells were excluded. (**D**) Parallel quantification of AxV binding and lectin binding to apoptotic lymphoblasts. UV-B-treated cells were stained by AxV or FITC-labelled lectins (MAL-I, SNA, UEA-I and GSL-II). AxV and lectin binding was quantified by flow cytometry after the indicated incubation periods. A decrease of MAL-I and SNA binding can be observed in parallel to a decrease of AxV negativity. Top: percentage of AxV-negative cells (AxV neg.). Lectin binding is quantified by mean fluorescence intensity (MAL-I, SNA, UEA-I, GSL-II). Values are means ± s.d. Statistical significance was calculated by Student's *t*-test and refers to the viable control; ***P<0.001, **P<0.01, *P<0.05.

Neuraminidase treatment reduces sialic acid residues on lymphoblasts without affecting their viability

We were interested in whether neuraminidase treatment influences the uptake of apoptotic cells by monocyte-derived phagocytes, to further estimate the role of Sias in the regulation of apoptotic cell engulfment. The neuraminidase we employed specifically cleaves α2,3-, α2,6- and α2,8-linked Sia residues. Apoptotic cells were treated by neuraminidase for the periods indicated in the figures

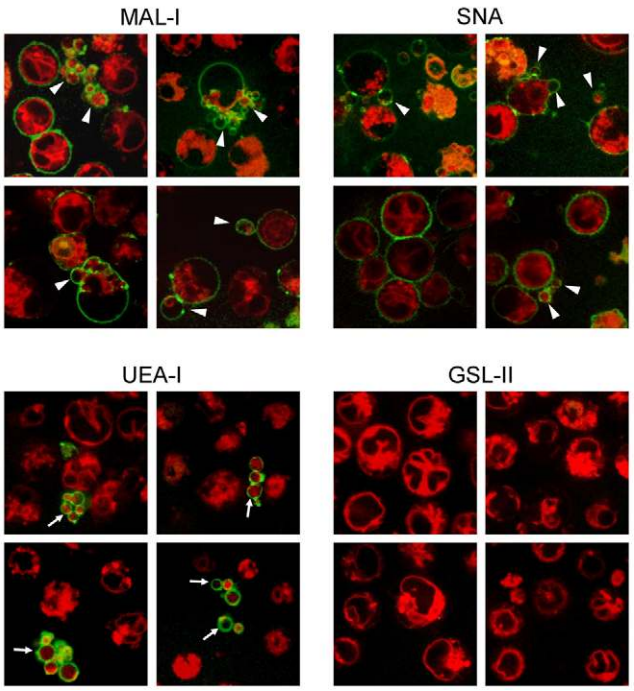

Fig. 2. Analysis of lectin binding to apoptotic lymphoblasts by means of confocal microscopy. Apoptosis was induced by UV-B treatment. Cell suspension containing apoptotic cells and apoptotic-cell-derived membrane blebs was stained by ER-tracker (red) and FITC-labelled lectins (green) 24 hours after apoptosis induction. Arrowheads show apoptotic cell blebbing; arrows point to UEA-I-stained apoptotic-cell-derived membrane blebs.

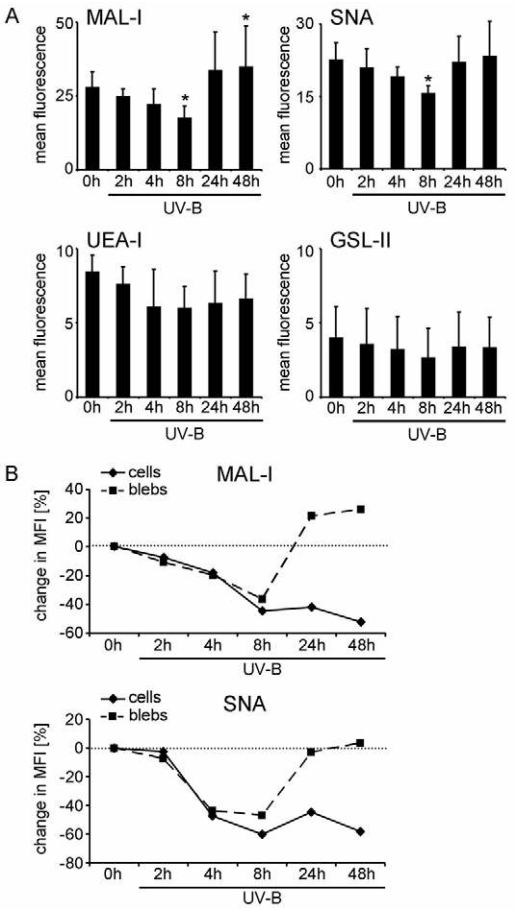

Fig. 3. Quantification of lectin binding to apoptotic-cell-derived membrane blebs. (**A**) Analysis of lectin binding to apoptotic-cell-derived membrane blebs. Apoptotic-cell-derived membrane blebs were stained by FITC-labelled lectins. Mean fluorescence intensity was quantified by flow cytometry after the indicated incubation periods. The bar graphs show the mean fluorescence intensity after staining by the indicated lectin (MAL-I, SNA, UEA-I, GSL-II). Values are means ± s.d. obtained from five independent experiments. Statistical significance was calculated by Student's *t*-test referring to the mean fluorescence intensity detected at 0 hours (*P<0.05). (**B**) Quantification of percentage change in sialic acids on the surface of apoptotic-cell-derived membrane blebs and apoptozing cells during the progression of apoptosis. The percentage change in mean fluorescence intensity (MFI) after MAL-I and SNA staining and flow cytometry (cf. Fig. 1D and Fig. 3A) was calculated in relation to the value obtained immediately after apoptosis induction (MFI at 0 hours). Values obtained at 0 hours were set at 0% change. Percentage change was calculated as MFI×100/MFI at 0 hours.

(Figs 5–9). SNA binding to untreated or neuraminidase-treated cells was quantified in order to verify the decrease of Sia residues after neuraminidase treatment. As shown in Fig. 5, neuraminidase caused a significant decline of Sia residues, which was obviously dependent on the duration of treatment.

It is essential to exclude the possibility that neuraminidase induces apoptosis, necrotic cell death, or an increase of PS exposure in order to substantiate the role of Sia exposure for the engulfment of apoptotic cells. Thus, in parallel to the described SNA-binding assay, cellular viability and PS exposure was assessed by AxV and PI staining. As shown in Fig. 5, neuraminidase treatment did not influence PS exposure.

Neuraminidase treatment enhances the uptake of apoptotic cells and apoptotic-cell-derived membrane blebs by monocyte-derived phagocytes

We next wanted to analyze whether desialylation influences the process of apoptotic cell engulfment. To this aim, neuraminidase-treated apoptotic cells and cell-derived membrane blebs were co-incubated with monocyte-derived phagocytes. Neuraminidase-treated apoptotic cells and blebs were washed before co-incubation (in the presence of heat-inactivated fetal bovine serum, FBS) in order to remove residual neuraminidase. Engulfment of apoptotic cells and apoptotic-cell-derived membrane blebs was quantified by flow cytometry. As shown in Fig. 6A, the engulfment of apoptotic cells was enhanced after neuraminidase treatment as compared to untreated cells. This effect was statistically significant if neuraminidase treatment was performed for 30 minutes. Similar results were obtained when analyzing the engulfment of neuraminidase-treated apoptotic-cell-derived membrane blebs (Fig. 6A).

We also performed confocal microscopy to discriminate between mere binding of apoptotic cells and blebs and an actual engulfment. As shown in Fig. 6B, an increased engulfment of apoptotic cells was detected employing confocal microscopy (see arrowheads in Fig. 6B). This increased engulfment of apoptotic cellular debris was all the more pronounced when analyzing apoptotic-cell-derived membrane blebs.

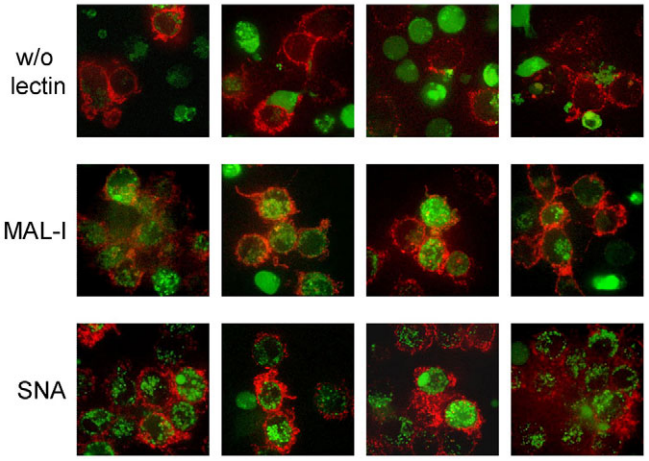

Fig. 4. Sialic-acid-binding plant lectins enhance the phagocytosis of apoptotic cells. Monocyte-derived phagocytes (stained by CD14-PE, shown in red) and UV-B irradiated (90 mJ/cm^2) apoptotic lymphoblasts (stained by CFSE, shown in green) were co-cultured for 24 hours. Before co-culture, lymphoblasts were incubated with the lectins MAL-I and SNA; untreated lymphoblasts (w/o lectin) served as controls. After 24 hours of co-culture cells, were analyzed by confocal microscopy.

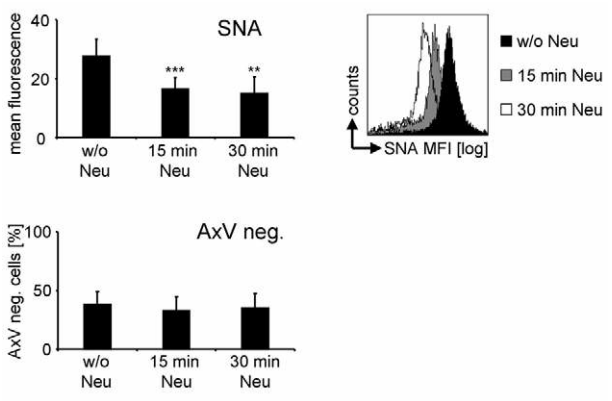

Fig. 5. Neuraminidase treatment causes a reduced binding of SNA to apoptotic lymphoblasts without affecting cellular viability. After apoptosis induction (UV-B, 90 mJ/cm^2), apoptotic lymphoblasts were treated with neuraminidase (Neu) for the indicated time periods. Staining by SNA was performed immediately after neuraminidase treatment. AxV and PI staining was done 24 hours after neuraminidase treatment. Top left: MFI after staining by SNA. Bottom left: percentage of AxV-negative and PI-negative cells. Values are means ± s.d. obtained from nine independent experiments. Statistical significance was calculated by Student's *t*-test and refers each to the preceding treatment; ***P<0.001, **P<0.01, *P<0.05. Right: original data of SNA fluorescence obtained from one representative experiment.

Monocyte-derived phagocytes show an altered cytokine release after engulfment of neuraminidase-treated cells and blebs

Apoptotic cells are reported to have anti-inflammatory effects. Macrophages incubated with apoptotic cells have been shown to secrete less pro-inflammatory and more anti-inflammatory cytokines (Voll et al., 1997). In the previously described experiments, we observed an increased engulfment of apoptotic cells and blebs if sialic-acid-specific lectins were bound or if Sias were cleaved by neuraminidase. Thus, we wondered whether these alterations of the glycocalyx also influence the response of monocyte-derived phagocytes to apoptotic cells and membrane blebs. To analyze this, we quantified cytokines in the supernatant of monocyte-derived phagocytes after co-incubation with apoptotic cells and apoptotic-cell-derived membrane blebs. As a control, monocyte-derived phagocytes were stimulated by LPS. LPS treatment considerably stimulated the release of the pro-inflammatory cytokines IL-6 and TNF-α, whereas no significant release of these cytokines was detected after the engulfment of apoptotic cells or blebs. A statistically significant increase in TNF-α as well as in IL-6 secretion was observed if apoptotic cells and blebs had been pretreated by neuraminidase. However, compared to the positive control (treated with lipopolysaccharide, LPS), neuraminidase-treated apoptotic cells and blebs can be considered as rather weak inducers of TNF-α or IL-6 release (Fig. 7). Analyzing IL-8 and IL-4 secretion, we observed a release of IL-8 and IL-4 if monocyte-derived phagocytes had engulfed apoptotic-cell-derived membrane blebs. However, neuraminidase treatment did not affect IL-8 secretion, and a slight decrease in IL-4 release was detected when apoptotic cells had been pretreated by neuraminidase (Fig. 7). We further analyzed IL-1β, IL-2, IL-5, IL-10, IL-12p70, IFN-γ in the supernatants of monocyte-derived phagocytes. Here, no significant changes were observed comparing untreated apoptotic cells and blebs and neuraminidase-treated apoptotic cells and blebs (not shown).

Monocyte-derived phagocytes show increased binding and uptake of neuraminidase-treated viable lymphoblasts

Having observed an increased engulfment of apoptotic cells and apoptotic-cell-derived membrane blebs after cleavage of Sias, we wondered whether neuraminidase treatment might also influence the interactions between viable lymphocytes and monocyte-derived phagocytes. Viable cells were treated with neuraminidase and the cleavage of Sias was confirmed analyzing the binding of SNA (Fig. 8A). Again AxV and PI staining were performed in parallel to exclude an induction of cell death (apoptosis or necrosis) by neuraminidase. Then, phagocytosis assays were performed, co-incubating monocyte-derived phagocytes together with viable lymphoblasts and neuraminidase-treated viable lymphoblasts, respectively. Interestingly, after neuraminidase treatment, the interactions between monocyte-derived phagocytes and lymphoblasts were enhanced and an engulfment of viable cells was even observed. Analyses by flow cytometry revealed increased interactions between neuraminidase-treated viable lymphoblasts and monocyte-derived phagocytes. However, this was not statistically significant (Fig. 8B). The effects of neuraminidase treatment were clearly detected by confocal microscopy. In these experiments we observed increased interactions between phagocytes and lymphoblasts, if the latter had been treated with neuraminidase. Furthermore, neuraminidase-treated lymphocytes interacting with monocyte-derived phagocytes clearly showed morphological changes, whereas non-interacting lymphocytes maintained their round shapes (arrowheads, Fig. 8C). Confocal microscopy confirmed the engulfment by phagocytes of neuraminidase-treated viable cells (arrows, Fig. 8C; enlarged sections 1–3, Fig. 8C).

Engulfment of resting peripheral blood lymphocytes after treatment with neuraminidase

In the previously described experiments we observed an enhanced engulfment of apoptotic and viable, activated lymphocytes. This engulfment was mediated and/or enhanced by surface desialylation.

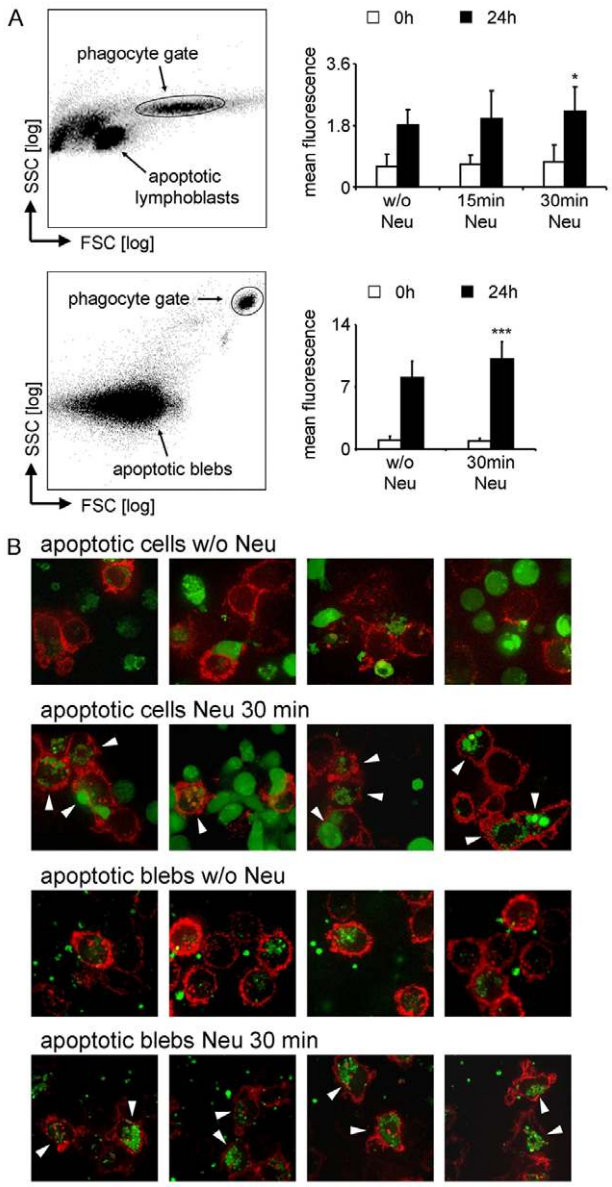

Fig. 6. Neuraminidase-treatment enhances uptake of apoptotic cells and apoptotic-cell-derived membrane blebs. (**A**) Monocyte-derived phagocytes were co-incubated with CFSE-labelled apoptotic cells or apoptotic-cell-derived membrane blebs. Left: dot plots show FSC/SSC properties of apoptotic cells, apoptotic blebs and phagocytes; the phagocyte gates are indicated. Right: bar graphs show mean fluorescence intensity (CFSE) gating on phagocyte population (phagocyte gate). Values are means ± s.d. of nine independent experiments. Statistical significance was calculated by Student's *t*-test and refers each to the untreated control; ***P<0.001, **P<0.01, *P<0.05. (**B**) Confocal microscopy images of anti-CD14-stained phagocytes and CFSE-stained apoptotic cells or apoptotic-cell-derived membrane blebs. Phagocytes are shown in red. CFSE-stained apoptotic cells or apoptotic-cell-derived membrane blebs are shown in green. Upper row: untreated lymphoblasts; second row, lymphoblasts after neuraminidase treatment for 30 minutes; third row, untreated apoptotic-cell-derived membrane blebs; bottom row, apoptotic-cell-derived membrane blebs after neuraminidase treatment for 30 minutes. Arrowheads indicate engulfed apoptotic cells or apoptotic-cell-derived membrane blebs.

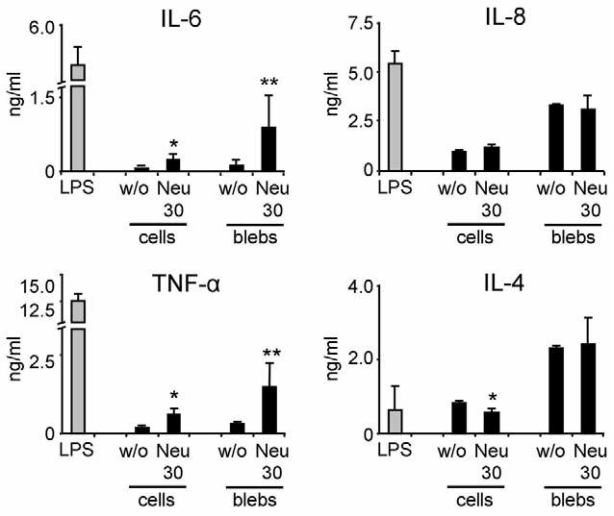

Fig. 7. Release of cytokines from monocyte-derived phagocytes after engulfment of neuraminidase-treated cells and blebs. Monocyte-derived phagocytes were co-incubated with apoptotic lymphoblasts (cells) or apoptotic-cell-derived membrane blebs. Apoptotic cells and apoptotic-cell-derived membrane blebs were treated by neuraminidase for 30 minutes (Neu 30). Untreated cells and membrane blebs served as controls (w/o). As a positive control for an inflammatory stimulus, monocyte-derived phagocytes were treated with LPS. Supernatants were harvested after 24 hours and cytokines were quantified by flow cytometry. The amount of cytokines detected in the cellular supernatants is shown in ng/ml. Values are means ± s.d. of five independent experiments. Statistical significance was calculated by Student's *t*-test and refers to the untreated control (w/o); **P<0.01, *P<0.05.

However, a slight increase in the exposure of *eat-me* signals, like PS, is not exclusively observed after apoptosis induction but can also occur after cellular activation. Thus, we wanted to substantiate the role of desialylation for the engulfment of resting peripheral blood lymphocytes (PBL). To this aim, apoptotic (UV-B treated) and viable PBL were treated by neuraminidase and co-incubated together with monocyte-derived phagocytes. Engulfment of PBL was quantified by flow cytometry as described above. Analyzing apoptotic PBL we detected an increased engulfment after neuraminidase treatment, as shown in Fig. 9 (upper graph). This increase appeared to be dependent on the duration of neuraminidase treatment and was statistically significant after treatment for 15 and 30 minutes. However, in contrast to the results obtained with activated lymphoblasts, neuraminidase treatment did not enhance the interactions between viable PBL and monocyte-derived phagocytes (Fig. 9, lower graph). These data suggest that changes in surface glycosylation can either directly mediate cellular engulfment or enhance phagocytosis by cooperation with further phagocytosis signals.

Discussion

Changes in the glycomic profile of apoptotic cells have previously been studied by various groups, who have analyzed cells of different origin (Azuma et al., 2002; Hart et al., 2000; Rapoport and Pendu, 1999). In these previous studies, both an increase and a decrease of membrane-bound Sias have been reported, depending on the cell type under investigation. We employed activated lymphoblasts to investigate surface changes during apoptosis. These cells are highly susceptible to apoptotic cell death and represent activated T-cells, which physiologically are eliminated in a great amount at the end of an immune response (Hieronymus et al., 2000). We observed a reduction of terminal α2,6-linked Sias (decreased

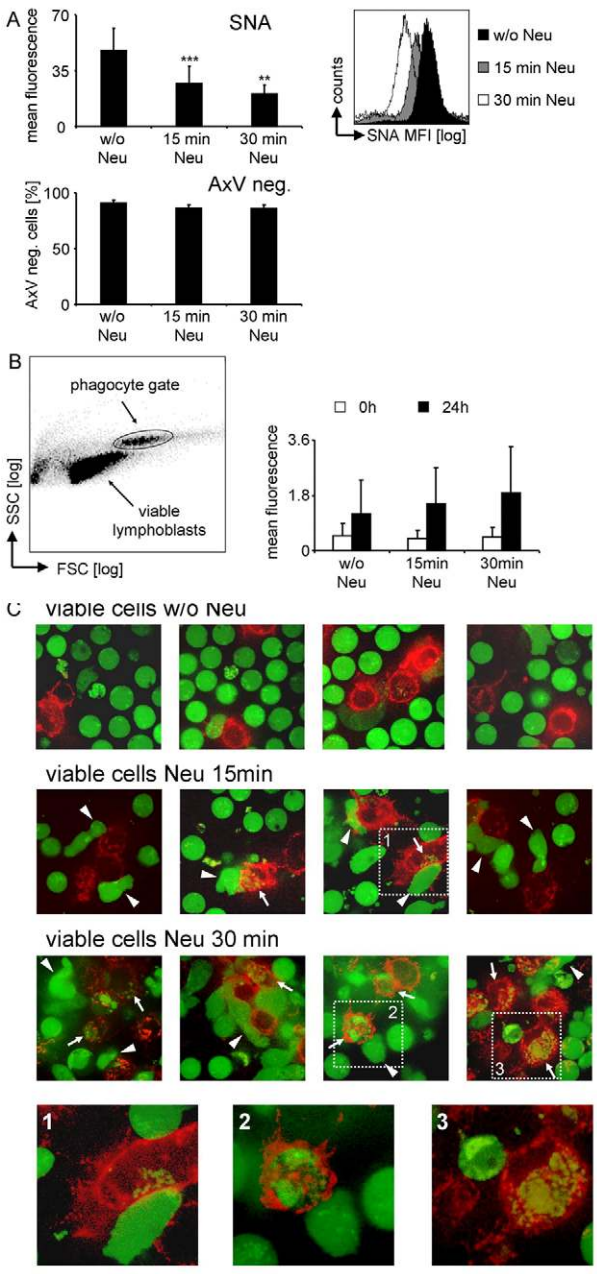

Fig. 8. Monocyte-derived phagocytes bind and engulf neuraminidase-treated viable lymphoblasts. (**A**) Viable lymphoblasts were treated with neuraminidase (Neu) for the indicated time periods. Staining by SNA was performed immediately after neuraminidase treatment. AxV and PI staining was performed 24 hours after neuraminidase treatment. Top left: MFI after staining by SNA. Bottom left: percentage of AxV-negative and PI-negative cells. Values are means ± s.d. obtained from nine independent experiments. Statistical significance was calculated by Student's *t*-test and refers to the preceding treatment; ***P<0.001, **P<0.01, *P<0.05. Right: original data of SNA fluorescence obtained from one representative experiment. (**B**) Monocyte-derived phagocytes were co-incubated with CFSE-labelled viable lymphoblasts. Left: FSC/SSC properties of phagocytes and viable lymphoblasts. Right: mean fluorescence intensity (CFSE) gating on phagocytes (phagocyte gate). Values are means ± s.d. of nine independent experiments. (**C**) Confocal microscopy images of anti-CD14-stained phagocytes and CFSE-stained lymphoblasts. Phagocytes are shown in red, lymphoblasts are shown in green. Upper row, untreated lymphoblasts; second row, lymphoblasts after neuraminidase treatment for 15 minutes; third row, lymphoblasts after neuraminidase treatment for 30 minutes; bottom row, enlarged sections (squares 1, 2, 3). Arrowheads indicate morphological changes of neuraminidase-treated (Neu) lymphoblasts interacting with phagocytes. Arrows indicate engulfed CFSE-positive material. Enlarged sections also show engulfed CFSE-positive material.

binding of SNA) as well as a reduction of Sias in α2,3-linkage to galactose (decreased binding of MAL-I) on the cellular surface during apoptosis (Fig. 1). An intracellular staining was excluded because only cells that maintained their plasma membrane integrity were analyzed. The high molecular mass of the lectins [SNA 240 kDa (Van Damme et al., 1996) and MAL 130 kDa (Kawaguchi et al., 1974)] renders a passive entrance unlikely, and confocal microscopy confirmed a membrane-associated fluorescence. Therefore, the loss of SNA and MAL-I staining can be attributed to a decrease of Sias on the outer leaflet of the plasma membranes. Analyzing apoptotic-cell-derived membrane blebs after induction of apoptosis, we observed an initial decrease of Sias. However, during later stages of apoptosis, MAL-I binding was enhanced (Fig. 3A,B).

The exact mechanisms underlying these changes in the glycomic profile remain elusive. One possibility is an increase in the activity of the endogenous cellular surface sialidase (NEU-3) (Azuma et al., 2000). Another model explains the surface changes in the glycomic profile during apoptosis by an exposure of immature membrane epitopes due to the redistribution of immature membranes into apoptotic-cell-derived membrane blebs (Franz et al., 2007). As we observed a prominent staining of apoptotic-cell-derived membrane blebs by SNA and MAL-I, the loss of α2,3- and α2,6-linked Sias might also be caused by apoptotic cellular membrane blebbing. Interestingly, after induction of apoptosis, exposure of Sias initially decreased on the surface of apoptotic blebs (at 2, 4 and 8 hours), whereas it was increased at later points of time during the progression of apoptosis. These data suggest that an increase in sialidase activity on the cellular surface during early apoptosis results in a decreased exposure of Sias on the cell surface. Consequently, blebs released by vesicle shedding from the cellular membrane also show a reduced exposure of Sias. In contrast to this, during later stages of apoptosis, a redistribution of immature (intracellular) membranes into apoptotic blebs might finally cause an increased exposure of Sias on the bleb surface. This scenario is supported by a previous publication by Franz and co-workers (Franz et al., 2007). However, further studies will be necessary to decipher the distinct mechanisms underlying the changes in the glycomic profile of apoptotic cells and blebs. In the context of apoptotic cell blebbing, an interesting observation was the exposure of fucose residues (bound by UEA-I) on the surface of apoptotic-cell-derived membrane blebs, whereas viable and apoptotic cells remained nearly unstained. This observation might be explained by the fact that fucose residues are usually not exposed in accessible terminal positions within the glycocalyx. Thus, a binding of lectins to these fucose residues might be sterically hindered. Changes of the glycocalyx of apoptotic membrane blebs might thus result in an accessible exposure of fucose residues, allowing the binding of UEA-I.

From studies on the clearance of red blood cells, it is known that a decrease of surface sialylation enhances the binding and uptake

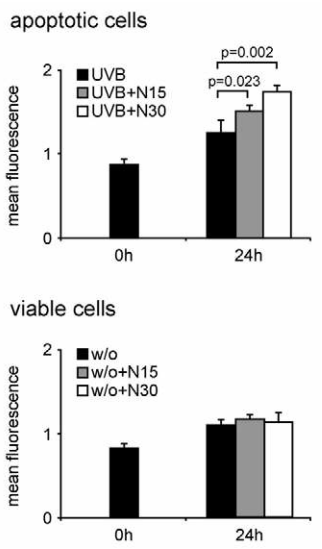

Fig. 9. Engulfment of neuraminidase-treated apoptotic and viable PBL by monocyte-derived phagocytes. Monocyte-derived phagocytes were co-incubated with CFSE-labelled apoptotic or viable PBL. PBL were treated with neuraminidase before co-culture. Neuraminidase treatment was performed for 15 minutes (N15) or 30 minutes (N30). Top: results obtained after coincubation of apoptotic PBL with phagocytes (UV-B + N15, UV-B + N30); UVB indicates untreated controls. Bottom: results obtained after coincubation of viable cells with phagocytes (w/o + N15, w/o + N30); w/o indicates untreated controls. The graphs show mean fluorescence intensity values (CFSE) gating on phagocytes. Values are means ± s.d. of three independent experiments. Statistical significance was calculated by Student's *t*-test.

by phagocytes of senescent erythrocytes (Bosman et al., 2005; Ensinck et al., 2006) and Sias have also been previously linked to apoptotic cell clearance (Fischer et al., 1991; Rapoport et al., 2005). Further studies will be needed to identify the receptors involved in the recognition of surface desialylation. The asialoglycoprotein receptor is one of the best-studied receptors for desialylated glycoproteins. However, its physiologic functions and the in vivo ligands are not clearly defined (Weigel and Yik, 2002). Beside this receptor, other molecules (e.g. CD43) that recognize changes in the cellular sugar coat have been described (Dini et al., 1992; van den Berg et al., 2001).

Co-incubation of apoptotic cells with the lectins MAL-I and SNA led to their highly enhanced uptake by phagocytes, suggesting an involvement of Sias in the regulation of phagocytosis. To further clarify this, neuraminidase-treated apoptotic lymphoblasts were co-cultured together with phagocytes. Neuraminidase treatment enhanced the uptake of apoptotic cells as well as apoptotic-cell-derived membrane blebs. These results were obtained by flow cytometry and confirmed by confocal microscopy (Figs 4–6).

We were also interested in whether a decrease of Sias on the cellular surface influences the immunological function of phagocytes after apoptotic cell engulfment. Apoptotic cell clearance physiologically results in a non-inflammatory response. We detected a somewhat increased secretion of IL-6 and TNF-α after neuraminidase pretreatment of apoptotic cells and blebs. Nevertheless, neuraminidase treatment caused only a minor increase in IL-6 and TNF-α secretion compared with the positive control (LPS). Apoptotic-cell-derived membrane blebs enhanced the secretion of IL-8 and IL-4, whereas neuraminidase treatment had no effect.

We studied the interaction between viable lymphoblasts and phagocytes in an autologous system to further substantiate the role of a decreased Sias exposure in the regulation of cell-to-cell communication or cellular engulfment. As expected, confocal microscopy showed that viable lymphoblasts and phagocytes barely interacted. Interestingly, we observed an increased binding of viable cells to phagocytes, and even an engulfment, after neuraminidase treatment. Moreover, lymphoblasts that were in contact with phagocytes showed morphological alterations whereas those that did not interact with phagocytes retained their round shape. It is important to note that neuraminidase itself did not induced apoptotic cell death nor other features of apoptosis like morphological alterations or PS exposure.

To evaluate whether enhancement of phagocytosis by desialylation is dependent on the cellular activation status, we also analyzed the engulfment of resting PBL after treatment by neuraminidase. An increased engulfment by phagocytes of apoptotic cells was observed if apoptotic PBL were pretreated with neuraminidase. However, neuraminidase treatment did not significantly influence engulfment of viable PBL. Thus, the regulation of cell engulfment by surface desialylation seems to be dependent on the cellular activation status, because we observed an engulfment of viable lymphoblasts after neuraminidase treatment but resting and neuraminidase-treated PBL were not engulfed.

Taken together, we have characterized changes in the glycomic profile on the surface of apoptozing lymphoblasts, depicted by a decrease in α2,3- and α2,6-linked Sias on the cellular surface. Furthermore, an exposure of Sia residues was detected on the surface of apoptotic-cell-derived membrane blebs with an initially decrease in Sia exposure. However, during later stages of apoptosis, a high exposure of Sias on the surface of apoptotic-cell-derived blebs was found. This might be explained by a redistribution of immature membranes into apoptotic blebs. The decreased exposure of Sias on the surface of apoptotic cells as well as on the surface of early released apoptotic blebs influences their engulfment by monocyte-derived phagocytes. Most interestingly, a cleavage of Sias from the surface of viable lymphoblasts also caused strong interactions between viable lymphoblasts and professional phagocytes. Analysis of resting PBL, however, showed that neuraminidase treatment only influenced uptake of apoptotic PBL, and that engulfment of viable PBL was not influenced.

We conclude that, during apoptotic cell death, changes in the glycocalyx play a key role in the recognition of apoptotic cellular debris and the engulfment of apoptotic material by surrounding phagocytes. This regulatory effect of surface desialylation obviously depends on cellular activation status. On the basis of the present data, it will be interesting to study the glycocalyx in pathological situations, e.g. in systemic lupus erythematosus, where a dysregulation of the clearance of apoptotic cell material is discussed as a major etiopathogenetic event.

Materials and Methods

Cell preparation and culture media

Heparinized venous blood was obtained from normal healthy volunteers after informed consent. Peripheral blood mononuclear cells (PBMC) were separated by density gradient centrifugation (LSM 1077) and washed twice with phosphate buffered saline (PBS). Cells were cultured in RPMI 1640 supplemented with 4 mM L-glutamine, 10 mM HEPES buffer, 100 U/ml penicillin, 100 μg/ml streptomycin (all reagents obtained from PAA, Pasching, Germany). RPMI 1640 was further supplemented with 10% (v/v) heat inactivated fetal calf serum (FCS) (Gibco-BRL, Eggenstein, Germany). Cell viability was assessed by trypan blue exclusion test. To obtain PBL, CD14-positive cells were depleted from isolated PBMC by magnetic cell sorting (Miltenyi, Bergisch Gladbach, Germany).

Generation of activated lymphoblasts

To generate lymphoblasts, PBMC were activated with 1 μg/ml phytohemagglutinin (PHA) (Sigma, Taufkirchen, Germany) and 10 U/ml IL-2 (Roche, Mannheim, Germany) for 5 days. Thereafter, cells were expanded with 10 U/ml IL-2 for another 2 days. Resulting lymphoblasts were extensively washed and cultured as indicated.

Induction of cell death and detection of apoptosis

Apoptosis was induced by UV-B irradiation with 90 mJ/cm^2 or incubation with 0.1 μM STS. To quantify the rate of apoptosis, cells were analyzed by flow cytometry. Amongst other features, apoptosis is characterized by blebbing of the cellular membrane, leading to a decrease in FSC and an increase in the SSC. For detection of PS exposure on the cell surface, staining with FITC-conjugated AxV (Böhringer, Mannheim, Germany) in combination with PI was performed. 200,000 cells were stained for 30 minutes at 4°C with 200 ng of AxV–FITC and 500 ng PI in 500 μl Ringer's solution. The samples were immediately analyzed by flow cytometry.

Isolation of apoptotic-cell-derived membrane blebs

After induction of apoptosis and incubation for 18 hours, the cell culture supernatant was collected. Two additional centrifugation steps (500 ***g*** for 5 minutes) were performed in order to remove remaining cells. The supernatant was then passed through a 1.2-μm non-pyrogenic, hydrophilic syringe filter. After centrifugation at 100,000 ***g*** for 30 minutes, the pellet containing apoptotic-cell-derived membrane blebs was harvested and used for further experiments.

Lectin binding assays

Flow cytometric analyses were performed using an EPICS XL flow cytometer (Coulter, Hialeah, FL) or FACS scan flow cytometer (BD Biosciences, Erembodegem, Belgium), counting at least 20,000 events. By use of the following FITC-labelled plant lectins, different sugar moieties on the cell surface were detected: Griffonia (bandeiraea) simplicifolia lectin II (GSL-II) for detection of *N*-acetylglucosamine; Ulex europaeus agglutinin I (UEA-I), which is specific for fucose residues; Sambucus nigra (elderberry) bark lectin (SNA), which binds terminal α2,6-linked Sia residues; Maackia amurensis lectin I (MAL-I), which binds to Sias-α2,3-Gal. Fluorescence-labelled lectins were obtained from Vector Laboratories (Burlingame, CA). We incubated 100,000 cells in 50 μl R10 with 1 μg lectin and 125 ng PI for 30 minutes at 4°C and immediately analyzed the probes by flow cytometry or confocal microscopy.

Neuraminidase treatment

Cells (1×10^6) were incubated in 200 μl Ringer's solution with 0.2 U neuraminidase V from *Clostridium perfringens* (Sigma, Taufkirchen, Germany) at 37°C for the indicated incubation periods. Cells were subsequently intensively washed with 1 ml R10. Controls were incubated in 200 μl Ringer's solution (without neuraminidase) and further treated exactly like the other samples.

In vitro phagocytosis of CFSE-labelled cells and apoptotic-cell-derived membrane blebs by monocyte-derived phagocytes

Cells were stained with carboxyfluorescein succinimidyl ester (CFSE, 3 μM) for 10 minutes at 20°C. Subsequently, CFSE-labelled apoptotic-cell-derived membrane blebs were isolated from the cellular supernatant of apoptotic lymphoblasts after 16 hours of incubation, as described above. Monocytes were isolated from peripheral blood by magnetic activated cell sorting (CD14-positive selection, Miltenyi, Bergisch Gladbach, Germany). CD14-positive cells were then cultured for 24 hours in the presence of granulocyte-macrophage colony-stimulating factor (GM-CSF; 100 U/ml) to emerge monocyte-derived phagocytes. CFSE-labelled cells and membrane blebs were co-incubated with monocyte-derived phagocytes (cultured for 24 hours). Phagocytes (1×10^6/ml) were cocultured together with 1×10^6/ml apoptotic cells (ratio 1:1). Isolated membrane blebs were quantified by measuring their DNA content by means of spectrophotometry. Apoptotic blebs (350 μg/ml DNA) were added to 1×10^6/ml phagocytes. Phagocytosis was analyzed by flow cytometry. Gating on the CFSE fluorescence of phagocytes was analyzed. Increased fluorescence intensity was detected if CFSE-labelled cells or apoptotic bodies had been engulfed. Further engulfment of apoptotic cells or apoptotic-cell-derived membrane blebs was assessed by confocal microscopy.

Confocal microscopy

For confocal microscopy, cells were harvested and transferred into glass-bottom chamber slides for analysis on a PerkinElmer Ultra-View spinning disc confocal on Nikon TE2000-E Ti inverted microscope by using a 100× oil-immersion lens [excitation at 488, 568, 647 nm; detection at 650 nm (shown red) and 488 nm (shown green)]. For lectin analysis on lymphoblasts, 200,000 cells were stained by 4 μg FITC-labelled lectins and 20 μM ER-Tracker Red (glibenclamide BODIPY TR) (Invitrogen, Paisley, UK) for 30 minutes at 4°C. Confocal microscopy was performed immediately after the staining procedure. For the analysis of phagocytosis, CFSE-labelled lymphoblasts and apoptotic-cell-derived membrane blebs were co-incubated for 24 hours with 200,000 monocyte-derived phagocytes. Apoptotic cells (1×10^6/ml) were cocultured together with 1×10^6/ml phagocytes (ratio 1:1). Apoptotic blebs (350 μg/ml DNA) were coincubated with 1×10^6/ml phagocytes. Phagocytes were stained with PE-labelled anti-CD14 antibody (BD Biosciences, San Jose, CA).

Quantification of cytokines in cellular supernatants

Supernatants of monocyte-derived phagocytes were harvested after 24 hours of incubation. Phagocytes, apoptotic cells and apoptotic-cell-derived blebs were prepared and co-incubated as described above. Phagocytes (1×10^6/ml) were cocultured together with apoptotic cells (1×10^6/ml) or apoptotic-cell-derived membrane blebs (350 μg/ml DNA). Cytokines were quantified using a FlowCytomix Kit (Bender MedSystems, Vienna, Austria). Following the manufacturers protocol, we detected IL-1β, IL-2, IL-4, IL-5, IL-6, IL-8, IL-10, IL-12p70, IL-17, IL-18, IFN-α, IFN-γ, TNF-α and TNF-β by flow cytometry.

Confocal microscopy was done at the Nikon Imaging Center at the University of Heidelberg. We acknowledge Dr U. Engel and Dr C. Ackermann for excellent technical support. R.B. and M.H. acknowledge the financial support of the bilateral German–Ukrainian grant UKR08/035. H.-M.L. and M.S. were supported by research grant from the German Research Foundation (project Lo437/5-3).

References

Allen, H. J., Johnson, E. A. and Matta, K. L. (1977). A comparison of the binding specificities of lectins from Ulex europaeus and Lotus tetragonolobus. *Immunol. Commun.* **6**, 585-602.

Ashwell, G. and Morell, A. G. (1974). The role of surface carbohydrates in the hepatic recognition and transport of circulating glycoproteins. *Adv. Enzymol. Relat. Areas Mol. Biol.* **41**, 99-128.

Azuma, Y., Taniguchi, A. and Matsumoto, K. (2000). Decrease in cell surface sialic acid in etoposide-treated Jurkat cells and the role of cell surface sialidase. *Glycoconj. J.* **17**, 301-306.

Azuma, Y., Inami, Y. and Matsumoto, K. (2002). Alterations in cell surface phosphatidylserine and sugar chains during apoptosis and their time-dependent role in phagocytosis by macrophages. *Biol. Pharm. Bull.* **25**, 1277-1281.

Beer, A., Andre, S., Kaltner, H., Lensch, M., Franz, S., Sarter, K., Schulze, C., Gaipl, U. S., Kern, P., Herrmann, M. et al. (2008). Human galectins as sensors for apoptosis/necrosis-associated surface changes of granulocytes and lymphocytes. *Cytometry A* **73**, 139-147.

Bosman, G. J., Willekens, F. L. and Werre, J. M. (2005). Erythrocyte aging: a more than superficial resemblance to apoptosis? *Cell. Physiol. Biochem.* **16**, 1-8.

Cambi, A. and Figdor, C. G. (2003). Dual function of C-type lectin-like receptors in the immune system. *Curr. Opin. Cell Biol.* **15**, 539-546.

Cline, A. M. and Radic, M. Z. (2004). Apoptosis, subcellular particles, and autoimmunity. *Clin. Immunol.* **112**, 175-182.

Crocker, P. R., Paulson, J. C. and Varki, A. (2007). Siglecs and their roles in the immune system. *Nat. Rev. Immunol.* **7**, 255-266.

Dini, L., Autuori, F., Lentini, A., Oliverio, S. and Piacentini, M. (1992). The clearance of apoptotic cells in the liver is mediated by the asialoglycoprotein receptor. *FEBS Lett.* **296**, 174-178.

Ensinck, A., Biondi, C. S., Marini, A., Garcia Borras, S., Racca, L. L., Cotorruelo, C. M. and Racca, A. L. (2006). Effect of membrane-bound IgG and desialysation in the interaction of monocytes with senescent erythrocytes. *Clin. Exp. Med.* **6**, 138-142.

Fadok, V. A., Bratton, D. L., Rose, D. M., Pearson, A., Ezekewitz, R. A. and Henson, P. M. (2000). A receptor for phosphatidylserine-specific clearance of apoptotic cells. *Nature* **405**, 85-90.

Fischer, C., Kelm, S., Ruch, B. and Schauer, R. (1991). Reversible binding of sialidase-treated rat lymphocytes by homologous peritoneal macrophages. *Carbohydr. Res.* **213**, 263-273.

Flotenmeyer, M., Momayezi, M. and Plattner, H. (1999). Immunolabeling analysis of biosynthetic and degradative pathways of cell surface components (glycocalyx) in Paramecium cells. *Eur. J. Cell Biol.* **78**, 67-77.

Franz, S., Herrmann, K., Furnrohr, B. G., Sheriff, A., Frey, B., Gaipl, U. S., Voll, R. E., Kalden, J. R., Jack, H. M. and Herrmann, M. (2007). After shrinkage apoptotic cells expose internal membrane-derived epitopes on their plasma membranes. *Cell Death Differ.* **14**, 733-742.

Harduin-Lepers, A., Vallejo-Ruiz, V., Krzewinski-Recchi, M. A., Samyn-Petit, B., Julien, S. and Delannoy, P. (2001). The human sialyltransferase family. *Biochimie* **83**, 727-737.

Hart, S. P., Ross, J. A., Ross, K., Haslett, C. and Dransfield, I. (2000). Molecular characterization of the surface of apoptotic neutrophils: implications for functional downregulation and recognition by phagocytes. *Cell Death Differ.* **7**, 493-503.

Hennigar, R. A., Schulte, B. A. and Spicer, S. S. (1986). Histochemical detection of glycogen using Griffonia simplicifolia agglutinin II. *Histochem. J.* **18**, 589-596.

Hieronymus, T., Blank, N., Gruenke, M., Winkler, S., Haas, J. P., Kalden, J. R. and Lorenz, H. M. (2000). CD 95-independent mechanisms of IL-2 deprivation-induced apoptosis in activated human lymphocytes. *Cell Death Differ.* **7**, 538-547.

Kawaguchi, T., Matsumoto, I. and Osawa, T. (1974). Studies on hemagglutinins from Maackia amurensis seeds. *J. Biol. Chem.* **249**, 2786-2792.

Knibbs, R. N., Goldstein, I. J., Ratcliffe, R. M. and Shibuya, N. (1991). Characterization of the carbohydrate binding specificity of the leukoagglutinating lectin from Maackia amurensis. Comparison with other sialic acid-specific lectins. *J. Biol. Chem.* **266**, 83-88.

Kottgen, E., Reutter, W. and Tauber, R. (2003). Human lectins and their correspondent glycans in cell biology and clinical medicine. *Med. Klin (Munich)* **98**, 717-738.

Kranich, J., Krautler, N. J., Heinen, E., Polymenidou, M., Bridel, C., Schildknecht, A., Huber, C., Kosco-Vilbois, M. H., Zinkernagel, R., Miele, G. et al. (2008). Follicular dendritic cells control engulfment of apoptotic bodies by secreting Mfge8. *J. Exp. Med.* **205**, 1293-1302.

Miguet, L., Pacaud, K., Felden, C., Hugel, B., Martinez, M. C., Freyssinet, J. M., Herbrecht, R., Potier, N., van Dorsselaer, A. and Mauvieux, L. (2006). Proteomic analysis of malignant lymphocyte membrane microparticles using double ionization coverage optimization. *Proteomics* **6**, 153-171.

Miyanishi, M., Tada, K., Koike, M., Uchiyama, Y., Kitamura, T. and Nagata, S. (2007). Identification of Tim4 as a phosphatidylserine receptor. *Nature* **450**, 435-439.

Monti, E., Preti, A., Venerando, B. and Borsani, G. (2002). Recent development in mammalian sialidase molecular biology. *Neurochem. Res.* **27**, 649-663.

Park, D., Tosello-Trampont, A. C., Elliott, M. R., Lu, M., Haney, L. B., Ma, Z., Klibanov, A. L., Mandell, J. W. and Ravichandran, K. S. (2007). BAI1 is an engulfment receptor for apoptotic cells upstream of the ELMO/Dock180/Rac module. *Nature* **450**, 430-434.

Rapoport, E. and Pendu, J. L. (1999). Glycosylation alterations of cells in late phase apoptosis from colon carcinomas. *Glycobiology* **9**, 1337-1345.

Rapoport, E. M., Sapot'ko, Y. B., Pazynina, G. V., Bojenko, V. K. and Bovin, N. V. (2005). Sialoside-binding macrophage lectins in phagocytosis of apoptotic bodies. *Biochemistry (Mosc)* **70**, 330-338.

Schiller, M., Bekeredjian-Ding, I., Heyder, P., Blank, N., Ho, A. D. and Lorenz, H. M. (2008). Autoantigens are translocated into small apoptotic bodies during early stages of apoptosis. *Cell Death Differ.* **15**, 183-191.

Sharon, N. and Lis, H. (2004). History of lectins: from hemagglutinins to biological recognition molecules. *Glycobiology* **14**, 53R-62R.

Tsuji, S., Datta, A. K. and Paulson, J. C. (1996). Systematic nomenclature for sialyltransferases. *Glycobiology* **6**, v-vii.

Van Damme, E. J., Barre, A., Rouge, P., Van Leuven, F. and Peumans, W. J. (1996). The NeuAc(alpha-2,6)-Gal/GalNAc-binding lectin from elderberry (Sambucus nigra) bark, a type-2 ribosome-inactivating protein with an unusual specificity and structure. *Eur. J. Biochem.* **235**, 128-137.

van den Berg, T. K., Nath, D., Ziltener, H. J., Vestweber, D., Fukuda, M., van Die, I. and Crocker, P. R. (2001). Cutting edge: CD43 functions as a T cell counterreceptor for the macrophage adhesion receptor sialoadhesin (Siglec-1). *J. Immunol.* **166**, 3637-3640.

Varki, A. (1993). Biological roles of oligosaccharides: all of the theories are correct. *Glycobiology* **3**, 97-130.

Voll, R. E., Herrmann, M., Roth, E. A., Stach, C., Kalden, J. R. and Girkontaite, I. (1997). Immunosuppressive effects of apoptotic cells. *Nature* **390**, 350-351.

Wang, W. C. and Cummings, R. D. (1988). The immobilized leukoagglutinin from the seeds of Maackia amurensis binds with high affinity to complex-type Asn-linked oligosaccharides containing terminal sialic acid-linked alpha-2,3 to penultimate galactose residues. *J. Biol. Chem.* **263**, 4576-4585.

Weigel, P. H. and Yik, J. H. (2002). Glycans as endocytosis signals: the cases of the asialoglycoprotein and hyaluronan/chondroitin sulfate receptors. *Biochim. Biophys. Acta* **1572**, 341-363.

Wu, Y., Tibrewal, N. and Birge, R. B. (2006). Phosphatidylserine recognition by phagocytes: a view to a kill. *Trends Cell. Biol.* **16**, 189-197.

Zanchetti, G., Colombi, P., Manzoni, M., Anastasia, L., Caimi, L., Borsani, G., Venerando, B., Tettamanti, G., Preti, A., Monti, E. et al. (2007). Sialidase NEU3 is a peripheral membrane protein localized on the cell surface and in endosomal structures. *Biochem. J.* **408**, 211-219.